COLLECTIVE EFFECTS STUDIES OF THE DOUBLE-DOUBLE BEND ACHROMAT CELL AT DIAMOND

E. Koukovini-Platia, L. Bobb, R.T. Fielder, R. Bartolini[1], Diamond Light Source, Oxfordshire, UK
[1]also at John Adams Institute, University of Oxford, UK

Abstract

One cell of the Diamond storage ring has been converted from a double bend achromat (DBA) to a double-double bend achromat (DDBA). After the successful installation and beam commissioning in November 2016, beam-based studies were done to assess the effect of the new cell on the single- and multi-bunch instabilities both in the transverse and longitudinal planes. These are compared with the impedance estimate carried out both numerically and analytically.

INTRODUCTION

Diamond synchrotron is a 3rd generation light source with an energy of 3 GeV, it consists of 24 straight sections and has a circumference of 561.57 m. Insertion device (ID) radiation sources provide intense photon beams to the users. Studies were done to reconfigure the DBA cell to include an extra ID between the two dipoles [1–3]. As a result of these studies, one cell of the Diamond storage ring was converted from a DBA to a DDBA structure. The successful beam commissioning took place in November 2016 [4]. The DDBA structure allowed the creation of a new straight section where an in-vacuum ID was installed during the machine shutdown in March 2017.

In the DDBA cell, magnets provide greater field gradients than normal with quadrupoles at 70 T/m gradient and sextupoles at 2000 T/m^2 second derivative (d^2B_y/dx^2) [5]. To achieve such gradients using conventional water-cooled copper windings and iron poles required the magnet aperture radius to be reduced resulting in a smaller cross-section of the vacuum vessel. The vacuum vessels following the dipole magnets are made of copper to dissipate the heat load from high synchrotron radiation, while stainless steel was used for the dipole vessels and through some of the sextupole magnets [6].

Beam-based measurements were done to infer the impedance contribution of the recently installed DDBA structure to transverse and longitudinal instabilities. Comparison with the numerical prediction from Computer Simulation Technology (CST) [7] as well as with the analytical estimate of the resistive wall is shown.

DDBA EFFECT ON SINGLE-BUNCH INSTABILITIES

Vertical Thresholds

The single bunch instability thresholds versus vertical chromaticity have been measured by gradually injecting current into a single bunch until the instability onset. The comparison of the vertical thresholds before (blue) and after (red) the installation of the DDBA cell is shown in Fig. 1 for a radio-frequency (RF) voltage of 2.5 MV and without transverse feedback. Insertion devices are closed to minimum gaps.
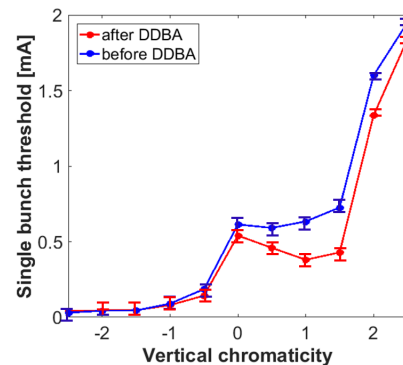
Figure 1: Vertical single bunch thresholds before (blue) and after (red) the DDBA cell installation as a function of chromaticity.

For positive chromaticity values, slightly lower single bunch thresholds are observed after the lattice modification of the DDBA cell, in agreement with expectations due to the increased impedance of the new cell.

Bunch Length and Energy Spread

The length of the electron bunch can be measured with a streak camera [8]. The streak camera records the electron bunch profile and with a Gaussian fit one can infer the r.m.s. bunch length. The measured bunch length as a function of single bunch current is plotted in Fig. 2. An increase of the bunch lengthening is observed after the DDBA installation, indicating an increased longitudinal machine impedance due to the new cell.

The energy spread measurements as a function of current were realised with 9 bunches uniformly spaced around the ring. For accurate measurements the pinhole cameras require a total current of at least 1 mA. Starting with 1 mA, more current was injected into the filled buckets until approximately 26.3 mA total current before the instability onset. The measurements before (blue) and after (red) the DDBA installation are shown in Fig. 3. No significant difference is observed due to the DDBA cell. The onset of the microwave instability is at around 2 mA, when the energy spread starts to increase. Below 1 mA, the data are still strongly affected by noise.
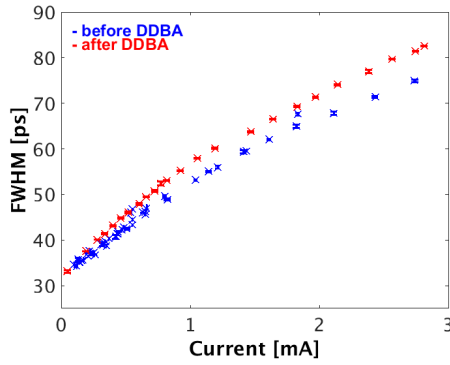
Figure 2: Bunch length measurements with a streak camera of the full width half maximum (FWHM) before (blue) and after (red) the DDBA cell installation as a function of single bunch current. The FWHM is calculated from the projection of the raw image from the streak camera.
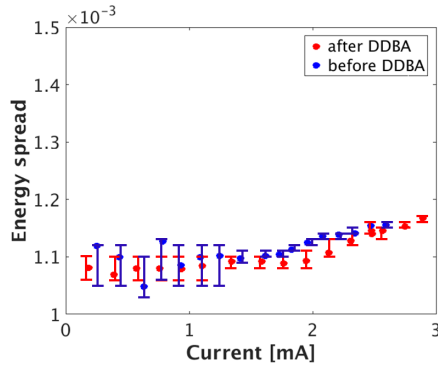
Figure 3: Energy spread measurements with the pinhole cameras before (blue) and after (red) the installation of the DDBA cell as a function of single bunch current. The microwave instability starts at around 2 mA causing increase of the energy spread.

Time Shift

The time shift $\Delta\tau$ of the centre of charge is related to the phase shift $\Delta\phi_s$ of the synchronous phase by the relation

$$\Delta\phi_s = \frac{2\pi}{T_{RF}}\Delta\tau, \qquad (1)$$

where T_{RF} is the period of the RF. The measurement of the time shift with current was done by injecting two bunches in the synchrotron on opposite sides of the ring. The first bunch is used as a reference for the phase with respect to the second bunch [9]. The current in the reference bunch is fixed to a small value of 0.8 mA, but big enough to be observed by the streak camera. Current is injected into the second bunch until the instability onset at around 2.6 mA.

The measurements of time shift versus single bunch current are shown in Fig. 4. Some increase is observed in the absolute time shift following the DDBA installation. This is due to the increased longitudinal loss factor, which can be
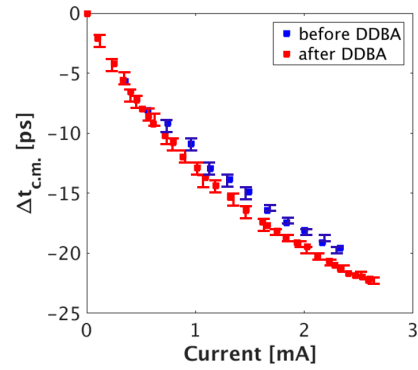
Figure 4: Time shift before (blue) and after (red) the installation of the DDBA as a function of single bunch current.

determined using the equation [9]

$$k \approx \frac{2\pi}{T_{RF}}\frac{eV_{RF}N_{ppb}}{q_{bunch}^2}\Delta\tau\cos(\phi_s), \qquad (2)$$

where e is the electron charge, V_{RF} is the RF voltage, N_{ppb} is the number of particles per bunch and q_{bunch} is the bunch charge. Using Eq. 2 and the measurements in Fig. 4, the loss factor can be determined as a function of current. As a second step, the single bunch current can be related to the bunch length via the measurements shown in Fig. 2. Finally the loss factor is plotted as a function of the r.m.s. bunch length in Fig. 5.
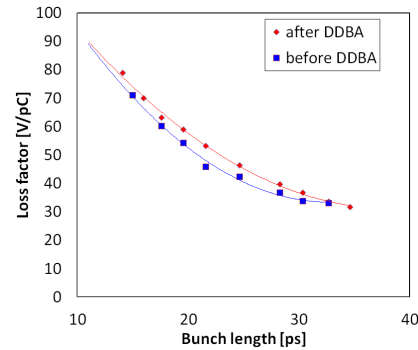
Figure 5: Loss factor before (blue) and after (red) installing the DDBA as a function of the r.m.s. bunch length.

For $V_{RF} = 2.5$ MV and insertion devices closed to minimum gaps the loss factor is around 89 V/pC for the zero-current bunch length of 12.2 ps with wigglers on after the installation of the DDBA, while it was around 88 V/pC before. The difference of 1 ± 0.3 V/pC can be largely attributed to the new cell.

CST simulations of each individual component of the DDBA such as dipole vessels, transitions, insertion device straight, beam position monitors, bellows, pumping ports etc., contribute to a total loss factor of 0.64 V/pC for the DDBA cell. Simulations and measurements are in reasonable agreement. The element-by-element contributions obtained using CST are shown in Fig. 6. All CST simulations have been done assuming nominal bunch length. The loss

05 Beam Dynamics and Electromagnetic Fields

D06 Coherent and Incoherent Instabilities - Measurements and Countermeasures

factor is calculated automatically in CST as the integral of the convolution of the wakefield with the bunch profile.
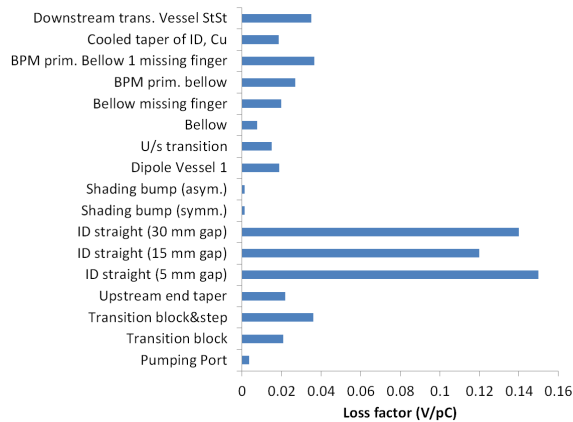
Figure 6: Simulations campaign with CST to calculate the loss factor of all major DDBA components.

DDBA EFFECT ON MULTI-BUNCH INSTABILITIES

Multi-bunch mode damping rates were measured before and after installation of the DDBA cell via grow-damp measurements with the transverse feedback [10]. These were fitted to the predictions of resistive wall impedance assuming the only change was to the effective mean vacuum chamber aperture. Differences in chamber material were neglected, while features such as tapers make calculating an exact average aperture difficult. Mean chamber apertures were found to reduce from 15.9 mm to 14.0 mm in the horizontal and from 12.0 mm to 10.3 mm in the vertical, resulting in an increased resistive wall impedance.

Simulations in CST did not predict any significant resonators would be added, and the measurements as seen in Fig. 7 and 8 support this as no new peaks are visible.
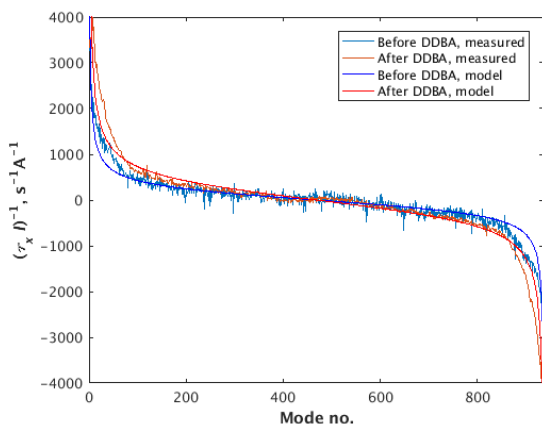
Figure 7: Horizontal damping rates before and after the DDBA installation versus the mode number. A comparison between measurements and the analytical prediction due to resistive wall impedance is shown.
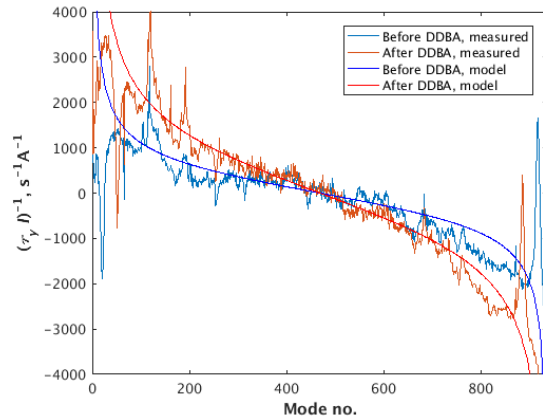
Figure 8: Vertical damping rates before and after the DDBA installation versus the mode number. Measured data are compared with the analytical prediction due to the resistive wall impedance.

CONCLUSION

Beam-based measurements of single- and multi-bunch effects in transverse and longitudinal planes have been compared before and after the installation of the DDBA cell. The DDBA cell is not transparent in terms of impedance as shown by the decrease of the single bunch thresholds, the increase in time shift and longitudinal loss factor, as well as the increase of resistive wall impedance. Further studies will be necessary in the scope of Diamond upgrade to ensure the desired machine performance.

ACKNOWLEDGEMENTS

REFERENCES

[1] R. Bartolini, and T. Pulampong, "Ultra-low emittance upgrade options for third generation light sources", in *Proc. IPAC'13*, Shanghai, China, May 2013, p. 237.

[2] R. Bartolini *et al.*, "Novel lattice upgrade studies for Diamond light source", in *Proc. IPAC'13*, Shanghai, China, May 2013, p. 240.

[3] R. Bartolini *et al.*, "Engineering integration constraints on the beam physics optimisation of the DDBA lattice for Diamond", in *Proc. IPAC'14*, Dresden, Germany, June 2014, paper MOPRO100.

[4] I.P.S. Martin *et al.*, "Electron beam commissioning of the DDBA modification to the Diamond storage ring", in *Proc. IPAC'17*, Copenhagen, Denmark, May 2017, paper WEPAB095, this conference.

[5] R.P. Walker *et al.*, "The double-double bend achromat (DDBA) lattice modification for the Diamond storage ring",

in *Proc. IPAC'14*, Dresden, Germany, June 2014, paper MO-PRO103.

[6] R.P. Walker *et al.*, "Preparations for the double-double bend achromat installation in Diamond light source", in *Proc. IPAC'16*, Busan, Korea, May 2016, paper WEPOW048.

[7] CST Particle Studio, , `http://www.cst.com`.

[8] C. Thomas, and G. Rehm, "Diamond optical diagnostics: first streak camera measurements", in *Proc. EPAC'06*, Edinburgh, Scotland, June 2006, paper TUPCH047.

[9] R. Bartolini, R. Fielder, and C. Thomas, "Loss factor and impedance analysis for the Diamond storage ring", in *Proc. IPAC'13*, Shanghai, China, May 2013, paper TUPWA052.

[10] R. Bartolini, R.T. Fielder, G. Rehm, "Multi-bunch instabilities measurement and analysis at the Diamond light source", in *Proc. IPAC'17*, Copenhagen, Denmark, May 2017, paper THPVA028, this conference.

05 Beam Dynamics and Electromagnetic Fields

D06 Coherent and Incoherent Instabilities - Measurements and Countermeasures